PERGAMON

International Journal of Heat and Mass Transfer 44 (2001) 3543–3551

International Journal of HEAT and MASS TRANSFER

www.elsevier.com/locate/ijhmt

Heat transfer and internal flow characteristics of a coil-inserted rotating heat pipe

Jin S. Lee, Chul J. Kim *

School of Mechanical Engineering, Sungkyunkwan University, 300 Chunchun-dong, Suwon 440-746, South Korea

Received 5 May 2000; received in revised form 11 October 2000

Abstract

To understand the flow pattern and the effect of a coil inside a cylindrical tube on the condensate flow, visualization and heat transfer performance tests were conducted. With the help of a coil inserted acryl tube, axial flow rates were measured to investigate the effect of coil helix angle, rotational speeds and fill charge rates. A coil-inserted tube showed a tendency of increasing the axial flow rates, especially at the pool regime. Also increasing the helix angle of coil resulted in the increase of flow rates and resulted in expediting the transition point of annular flow regime. The pumping effects for RHP with an inserted coil resulted in the enhancement of both condensation heat transfer coefficient and heat transport limitation, as obtained in the case of using internal fins. But these effects weakened in the range of higher rotational speeds with the transition of flow regime to annular flow. © 2001 Published by Elsevier Science Ltd.

1. Introduction

The rotating heat pipe (RHP) and its operating principle were first reported by Gray [1] in 1969. Normally, the RHP has no internal wick. However, the condensate can be returned more stably than the capillary heat pipes due to the centrifugal acceleration. In this sense, the RHP can effectively remove the heat conducted from the rotors of electric machinery. So far, many investigations have been reported on the performance enhancement of electric machinery by utilizing the RHP [1–5]. Vapor and liquid flow patterns inside the RHP depend on both rotational speed and internal geometry.

For the circular RHP, it was reported that the pool flow was observed in the low rotational speed while the annular flow appeared in the high speed range [6,7]. Fig. 1 shows these two flow patterns. At pool flow regime, liquid flow is predominantly effected by gravitational force, so is most of the liquid is located in the lower part of the pipe. As the rotational force increases, liquid film is formed uniformly by the centrifugal force, and the annular flow regime is established. Also, both the boiling/condensing heat transfer coefficients and the flow rate of the condensate have been reported to be the most important factors in the performance enhancement of the RHP.

On the other hand, there have been many investigations on the optimum charge of working fluid. As the charge increases, larger inclination angle of the vapor–liquid interface can be obtained. This results in the enhancement of dry-out limitation due to the increased liquid flow rate. However, it is important that overcharging leads to thicker liquid layer in the condenser and causes lower thermal conductance [7–9]. In this respect, much more accurate analysis and measurement are required to determine the optimum charge. A spiral fin was proposed to be installed internally by Marto et al. [10] and about 200–300% increase in the heat transport capacity was obtained since the liquid flow rate was significantly increased by the fin. Also, an internal groove [11] was proposed to take advantage of the capillary pressure in addition to the centrifugal pumping pressure. Marto [12] reported that axially tapered geometry (with 1–3°) resulted in the increase of the dry-out limit and performance enhancement. Lin [13] arranged the inner diameter of the evaporator to be larger than

* Corresponding author. Tel.: +82-31-290-7434; fax: +82-31-290-5849.

E-mail address: cjkim@me.skku.ac.kr (C.J. Kim).

0017-9310/01/$ - see front matter © 2001 Published by Elsevier Science Ltd.
PII: S0017-9310(00)00317-3

Nomenclature

Fr	Froude number ($R\omega^2/g$)
h	heat transfer coefficient (W/m^2 K)
m	mass flow rate (ml/s)
HP	heat pipe
N	rotational speed (rpm)
Q	heat transfer rate (W)
q''	heat flux (kW/m^2)
R	radius of pipe (mm)
RHP	rotating heat pipe
T	temperature (°C)
t	time (min)

Greek symbols

α	coil helix angle (°)
Ψ	fill charge ratio (%)
ω	angular velocity (rad/s)

Subscripts

a	adiabatic
c	condenser
e	evaporator

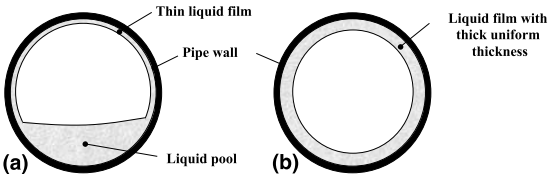

Fig. 1. Flow patterns of two-phase flow in a horizontal rotating heat pipe with a circular cross-section: (a) pool flow regime; (b) annular flow regime.

that of the other part in order to expedite pumping capability and retard the dry-out phenomenon occurring in the evaporator. Shimizu and Yamazaki [14] performed similar investigations using a typical coil (with 50 mm pitch and 10 mm height), and performance enhancement was observed in the range of low rotational speeds (50–400 rpm).

In the current study, a spiral coil was installed at the internal wall of the similar type of the RHP proposed by Marto. Concentration was made on the investigation to examine the effect of a coil on the enhancement of heat transport. For this purpose, experimental investigations were performed to measure the heat transport of the RHP (Fig. 2) with a spiral coil ($\Phi = 1.5$ mm). As reported in the previous studies, performance enhancement was observed in the low rotational speed, but no experimental result was reported for the range of high rotational speeds. From this respect, flow visualization experiments were first conducted for the rotational speeds ranging from 300 to 1650 rpm in order to examine the effect of rotational speed on the flow characteristics, and secondly, the heat pipe experiments were performed to investigate heat transfer characteristics encountered in the present RHP with the spiral coil represented in Fig. 2.

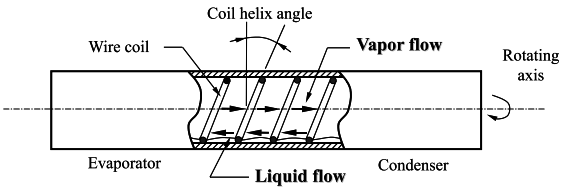

Fig. 2. A rotating heat pipe with a coil-insert.

2. Experimental apparatus and procedure

2.1. Apparatus for flow visualization and measuring flow rates

As shown in Fig. 3, a flow visualization device was constructed to examine the effect of spiral coil on the flow pattern and consisted of a transparent plastic tube, a supporting table and a speed control unit. The transparent tube was assembled with a spiral coil (stainless steel, $\Phi = 1.5$ mm) and connected to the flexible coupling installed at the end of the motor shaft. An AC motor and an inverter were used to control the rotational speed of the tube. As working fluid for flow visualization, water was supplied to the transparent tube.

The other end of the test device was open and connected to the collecting tank to measure the pumping flow rate developed by the rotating spiral coil. In flow visualization experiments, the pumping flow rate was measured with the variation of rotational speed, charge

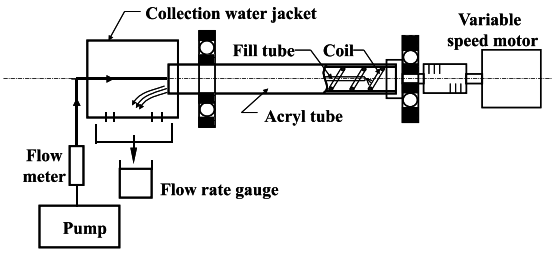

Fig. 3. Apparatus to visualize flows inside a rotating pipe equipped with a coil insert and measuring pumping flow rates.

ratio and helix angle. Experimental procedure can be summarized as follows.

First, water was supplied at constant rate for the certain rotational speed. The supply rate was measured at steady-state, i.e., the supply rate was identical to the discharge rate. Secondly, the charge ratio was determined by measuring the amount of water inside the tube. The supply rate corresponds to the liquid pumping rate due to the centrifugal acceleration in a real RHP. Charge ratio was estimated by measuring the amount of liquid remaining in the tube. In order to investigate the effect of spiral coil on the flow characteristics, the transparent tube with both ends closed was charged with water. The flow patterns were examined with the variation of rotational speed and charge ratio. For the low rotational speed, the liquid existed in the form of a pool, and the length of the pool was measured as a function of rotational speed for different values of charge ratio. As rotational speed increases, transition in the flow pattern occurred and the pool pattern changed to the annular regime. The rotational speed corresponding to the transition was also measured in the same way.

2.2. Apparatus for heat pipe thermal performance

In most cases, the diameter of the motor shaft is 25–40 mm, so a heat pipe with 20–30 mm diameter can be installed in the center of the shaft. Specifications of the RHP were summarized in Table 1. The inner diameter is 25.5 mm and total length is 360 mm. Both the evaporator and condenser parts are 300 mm long, and the length of the adiabatic part is 60 mm. The RHP was made of copper, and water was used as working fluid. Based on the coil geometry and charge ratio, four different heat pipes were constructed as shown in Table 1.

A schematic diagram of the experimental apparatus is represented in Fig. 4. The test apparatus consists of a heat pipe, an AC motor with an inverter, heating and cooling units, and a data logger. An electric heater (Nichrome wire: 7 Ω/m) was installed to produce a uniform heat flux on the outer surface of the evaporator. Electric power was supplied to the rotating heater by using a conducting brush made of a copper plate (thickness: 0.2 mm, width: 10 mm). To minimize heat loss, the heater was surrounded by insulating materials (Glass fiber: 20 mm thick).

The heat transported from the evaporator was removed by the coolant flowing through a coolant distributor installed in the condenser. A constant temperature bath was used to control the coolant temperature and flow rate. For the purpose of uniform cooling in the condenser, the coolant flow was divided by the intermittent holes (1.5 mm diameter, 10 mm in axial pitch) located in the inlet manifold (10 mm diameter). Wall temperature was measured at eight locations along the RHP using the T-type thermocouples with slip rings (SR20M). Two locations were assigned in the adiabatic region and three were in the evaporator and condenser, respectively. In the present experiment, the rotational speed was varied from 300 to 1650 rpm, and heat flux was adjusted from 1 to 30 kW/m^2.

3. Results and discussion

3.1. Pumping effect of a coil-inserted tube

According to the experimental results (for a typical RHP, 30 mm diameter) reported by Katsuta et al. [7], the liquid flow was characterized as the "Pool flow" in the low rotational speed since the liquid motion was dominated by the gravitational force. However, in the high rotational speed, the centrifugal force became dominant and the liquid flow was represented by "Annular flow". In the current experiment, the spiral coil functioned as an impeller to expedite the axial liquid flow in the low speed, as was the same trend for the case of a spiral fin proposed by Nakayama et al. [9]. This phenomenon occurred only in the low speed, and no axial liquid motion was observed in the annular flow (characterized as solid body rotation) which appeared in the relatively high rotational speed. Fig. 5 shows internal flow patterns and axial flow effect by the inserted coil tube ($\alpha = 15°$, $\Psi = 25\%$). As shown in Fig. 5(a), the liquid is accumulated at the bottom of right-hand side due to the liquid pumping of the spiral coil in low rotational speed (300 rpm). As the rotational speed increases, this trend becomes more significant as indicated in Figs. 5 (b) and (c). When the speed increases up to the point of transition, Fig. 5(d) shows the liquid flow pattern at the point of transition from the pool flow to the annular flow. The liquid pool accumulated in the

Table 1
Specification of the heat pipes designed and manufactured for the present experiment

Component	Material	Geometric dimension and fill charge ratio
Container	Copper	Inner diameter: 25.5 mm, outer diameter: 28.5 mm, length of eva. (con.): 150 mm, length of adia.: 60 mm
Working fluid	Water	Purity: 99.99%
Insert coil	Stainless steel	HP1: $\alpha = 22°$, $\Psi = 30\%$, HP2: $\alpha = 45°$, $\Psi = 30\%$, HP3: $\alpha = 45°$, $\Psi = 15\%$, HP4: $\alpha = 45°$, $\Psi = 7\%$

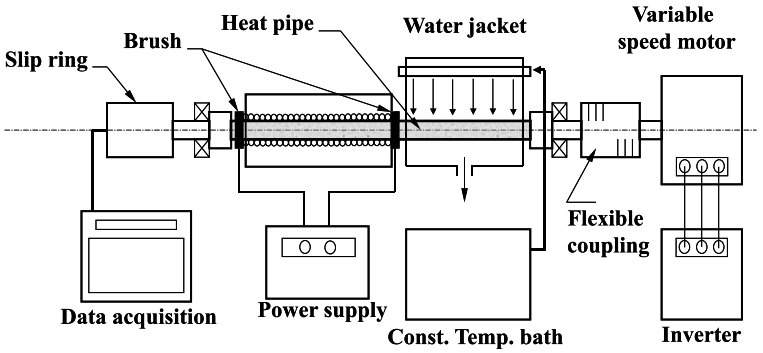

Fig. 4. Schematic diagram of the experimental apparatus for performance test of a rotating heat pipe.

right-hand side begins to disappear and move towards the left-hand side of the RHP.

As noted earlier, the axial flow rate was measured using the experimental device shown in Fig. 3. Figs. 6 and 7 represent variation of the axial flow rate as a function of charge ratio for the three different values of the helix angle (no coil, 15° and 45°). As shown in Fig. 6, the axial flow rate for the pool flow (300 rpm) tends to linearly increase with increase in the charge ratio. For the same charge ratio (10–30%), axial flow rate is enhanced up to 200–300% in the presence of the spiral coil, but the effect is not significantly changed by the magnitude of the helix angle. Fig. 7 shows the axial flow rate for the annular flow (1500 rpm). Overall trend of the axial flow rate versus charge ratio indicates that the effect of the helix angle on the enhancement of pumping capability becomes more significant as charge ratio increases.

3.2. Heat transfer coefficient

Normally, wall temperature of the evaporator and condenser is maintained constant in the axial direction when a heat pipe operates in the steady-state. Fig. 8 shows the axial distribution of wall temperature for the pool flow (300 rpm) and the annular flow (1500 rpm).

Overall trend indicates that both the evaporator and condenser are assumed to be maintained at the constant temperature regardless of the axial temperature deviation (1–2°C). From the results of the temperature measurements, both average evaporating and condensing heat transfer coefficients can be obtained as indicated in Eqs. (1) and (2).

$$h_e = \frac{Q_{out}}{A_e(T_e - T_v)}, \tag{1}$$

$$h_c = \frac{Q_{out}}{A_c(T_v - T_c)}. \tag{2}$$

Here, T_e and T_c represent the average evaporating and condensing wall temperature, respectively, and T_v, the vapor temperature, corresponds to the average vapor temperature of the adiabatic region. Q_{out} is the heat rejected from the condenser and expressed as:

$$Q_{out} = mC_p(T_{out} - T_{in}). \tag{3}$$

Here, m and C_p indicate the coolant mass flow rate and specific heat, respectively. T_{in} is the coolant inlet temperature, and T_{out} is the coolant outlet temperature.

It was reported that the most important factor governing the heat transfer coefficient of the RHP was the liquid flow pattern [7,9,11]. In the present experiments, rotational speed, charge ratio and helix angle were found as important parameters. Based on the results of the flow visualization experiments, the heat transfer coefficient was examined in terms of these parameters.

In Fig. 9, the heat transfer coefficient is represented as a function of rotational speed (300–1650 rpm) for the given conditions ($q'' = 17$ kW/m^2, $\Psi = 30\%$, $\alpha = 45°$ (HP1), 22° (HP2)). Both the evaporating and condensing heat transfer are estimated to be nearly the same as 500–700 W/m^2 K in the annular flow regime. Also, the effect of helix angle on the transition speed (rpm) is presented in Fig. 9 from the viewpoint of heat transfer coefficient. The transition point shifts from 1200 rpm to 700–800 rpm as the helix angle changes from 22° to 45°. This is the same trend observed in the flow visualization experiments. With increase in the helix angle, the transition tends to occur at the lower rotational speed as shown in Table 2.

At this point, the order of magnitude of the heat transfer coefficient with a coil needs to be compared with that corresponding to no coil. According to Lee [15], the average heat transfer coefficient without a coil was reported to be approximately 2000–4000 W/m^2 K in the pool flow regime and well matched with the analytical results of Semena and Khmelev [6].

In addition, in the annular flow regime, the average heat transfer coefficient decreased significantly (500–700

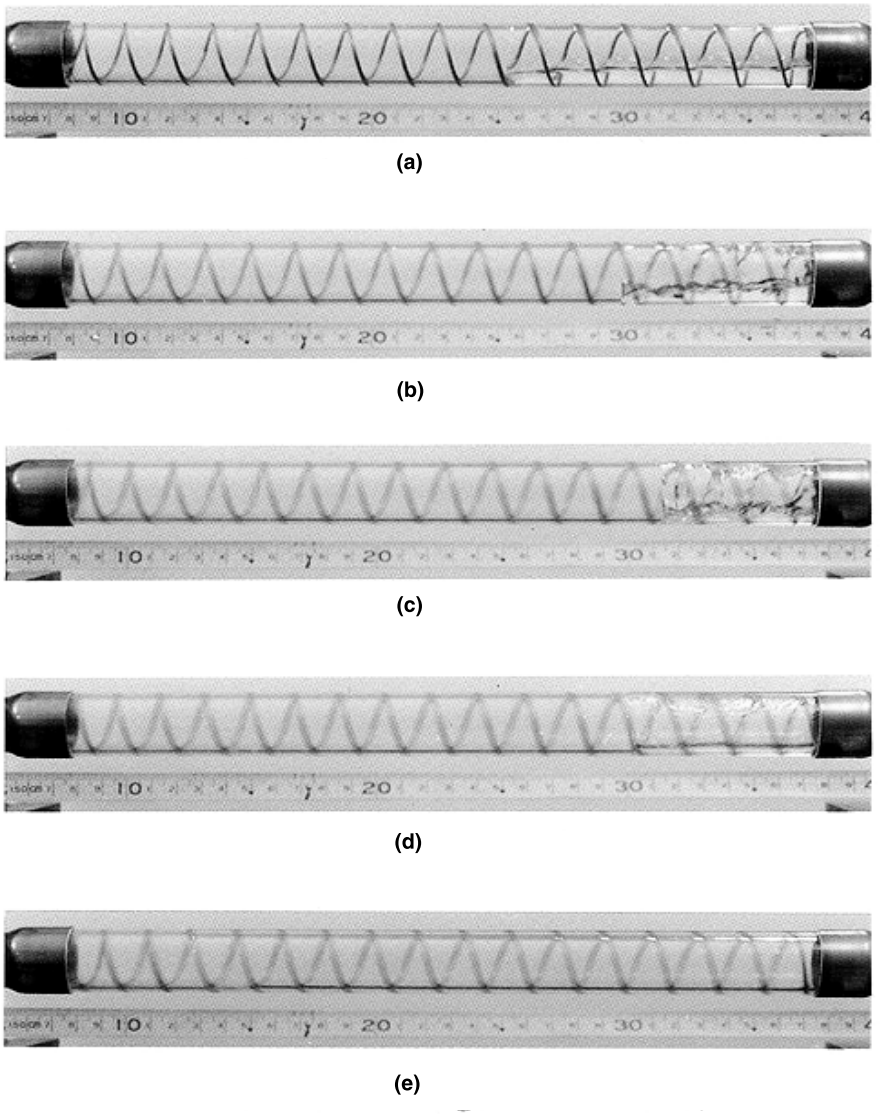

Fig. 5. Flow patterns inside a coil-inserted tube for several different values of rpm (wire coil helix angle: $\alpha = 15°$, fill charge ratio: $\Psi = 25\%$): (a) pool regime (300 rpm); (b) pool regime (900 rpm); (c) pool regime (1200 rpm); (d) transition to annular flow regime (1260 rpm); (e) annular flow regime (1260 rpm).

W/m^2 K) and approached the analytical results of Vasiliev and Khrolenok [16]. The order of magnitude of the average heat transfer coefficient (with a coil) in the pool flow can be estimated from Fig. 9 as, $h_e = 2800$–5000 W/m^2 K, $h_c = 1000$–4000 W/m^2 K. This indicates that the evaporating heat transfer coefficient is not much enhanced even if a coil is inserted inside the heat pipe. However, the enhancement is significant in the condenser due to the reduction of film thickness of the annular flow, as observed in the flow visualization experiments. In the evaporator, slight changes in the thickness of the liquid film do not seem to significantly affect the evaporating heat transfer coefficient. This phenomenon can be theoretically verified by considering the experimental correlations proposed by Vasiliev and Khrolenok. The evaporating heat transfer coefficient was dependent on the heat flux and the Froude number as shown in Eqs. (4) and (5). Charge ratio, regarded as an important parameter governing film thickness, was not included in the correlations

$$h_e = 440 q^2 Fr^{0.3} \text{ (undeveloped nucleate boiling)}, \quad (4)$$

$$h_e = 4.4 q^{0.68} \text{ (developed nucleated boiling)}. \quad (5)$$

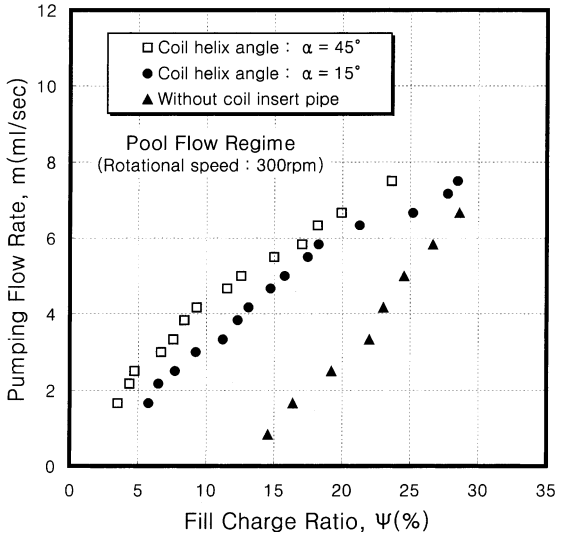

Fig. 6. Variations of axial flow rate of water with fill charge ratio Ψ at pool flow regime (rotational speed: 300 rpm).

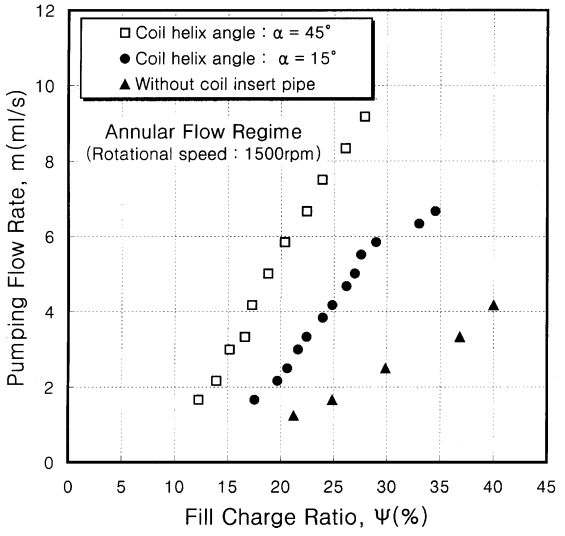

Fig. 7. Variations of axial flow rate of water with fill charge ratio Ψ at pool flow regime (rotational speed: 1500 rpm).

On the other hand, the evaporating and condensing heat transfer coefficients in the annular flow are $h_e = 700$–800 W/m^2 K and 400–600 W/m^2 K, respectively. The heat transfer coefficient is nearly unchanged when compared with those values corresponding to the case of no coil [14]. Although the liquid flow rate is significantly increased by means of a coil, this positive effect seems to be cancelled by the increase of the film thickness in the evaporator.

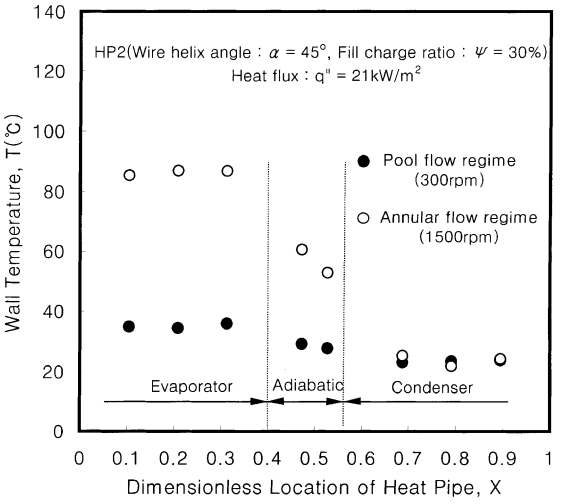

Fig. 8. Axial temperature distribution on the wall of the HP2, when two different flow regimes were established pool regime and annular regime (coil helix angle: $\alpha = 45°$, fill charge ratio: $\Psi = 30\%$).

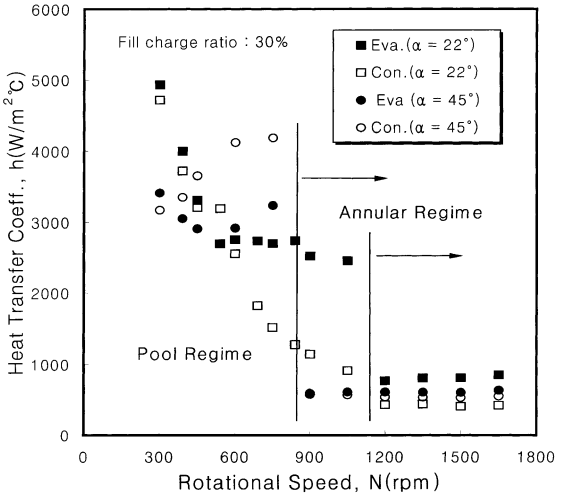

Fig. 9. Variations of heat transfer coefficient as both evaporator and condenser, when rotational speeds were increased stepwise up to 1700 rpm for HP1, HP2 (coil helix angle: $\alpha = 22°$, 45°, fill charge ratio: $\Psi = 30\%$, heat flux: $q'' = 17$ kW/m^2).

For two different values of charge ratio (15% and 30%), the heat transfer coefficient is represented as a function of rotational speed, as shown in Fig. 10. Overall trend indicates that the transition occurs at the lower rotational speed as the charge ratio decreases. Transition speed varies from 800–900 rpm to 600–700 rpm as the charge ratio changes from 30% to 15%. When the charge ratio is 15%, the condensing heat transfer

Table 2
Transient rotational speed for various heat pipes

Type of heat pipe (fill charge ratio: $\Psi = 30\%$)	Range of transient rotating speed (rpm)
Without coil insert [14]	1500–1700
HP1 ($\alpha = 22°$)	1000–1200
HP2 ($\alpha = 45°$)	800–900

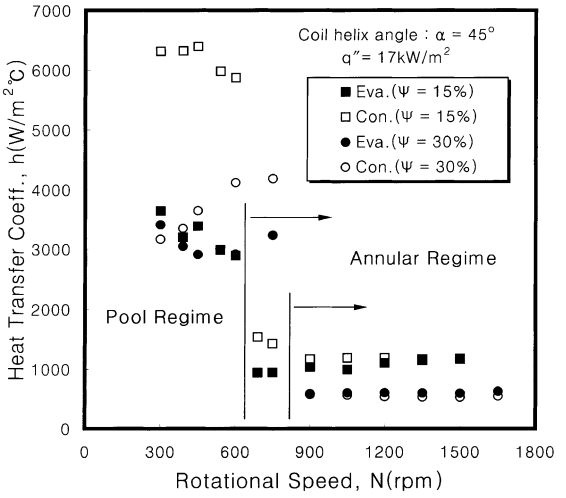

Fig. 10. Variations of heat transfer coefficient as both evaporator and condenser, when rotational speeds were increased stepwise up to 1700 rpm for HP2, HP3 (coil helix angle: $\alpha = 45^{\circ}$, fill charge ratio: $\Psi = 15$, 30%, heat flux: $q'' = 17$ kW/m^2).

coefficient is approximately twice greater than the evaporating heat transfer coefficient ($h_c = 6100$ W/m^2 K, $h_e = 3300$ W/m^2 K) in the pool flow. This phenomenon typically observed in the low level of charge ratio may be caused by the relatively thinner film thickness of the condenser when compared with that of the evaporator. However, when the charge ratio increases up to 30%, the condensing heat transfer approaches the evaporating heat transfer coefficient. The two heat transfer coefficients could be the same in the order of magnitude if the charge ratio becomes larger than 30%.

However, overall trend of heat transfer coefficient in the annular flow is quite different from that of the pool flow. Both the evaporating and condensing heat transfer coefficients tend to be kept constant and have same values. This can be explained by the uniform film thickness developed in the annular flow regime, as discussed in the results of flow visualization. Still, larger values are observed in the case of lower charge ratio. This trend of heat transfer coefficient can be identically observed in any annular flow regardless of the spiral coil. The optimum charge can be determined by using the previous analytical and experimental results for the case of no coil [7,9,16]. So, 15–30% of charge ratio can be regarded as an optimum level of charge even in the case of the spiral coil.

3.3. Heat transport limitation

In usual, the heat transport per unit area of an RHP is lower than that of a stationary heat pipe. So, the heat transport limitation of an RHP is determined by the heat rejected from the condenser at the moment of dry-out occurring at the end of the evaporator. In order to retard the dry-out phenomenon, numerous investigations are being conducted to examine the effects of important parameters such as charge ratio and configuration of the inner wall. Fig. 11 shows temporal variation of the wall temperature at the moment of dry-out, when the heat flux is increased from 2 to 3.7 kW/m^2. Temperature measurements for T1, T2 and T3 were made at the three locations, $x = 20$, 75 and 130 mm from the end of the evaporator, respectively. It is observed that T1, T2 and T3 increase continuously with time.

In the present study, the heating heat flux ranging from 5 to 40 kW/m^2 does not reach the critical heat flux if the charge ratio is larger than 15% recommended to

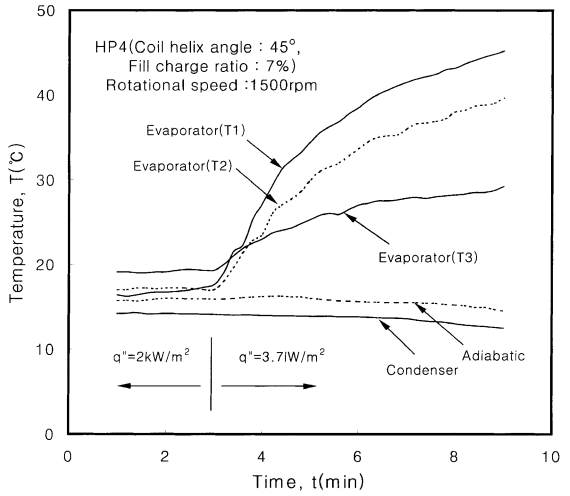

Fig. 11. Temperature rise due to local dry-out on the surface of evaporator, caused by deficit of condensate flow running down for the evaporator, when heat flux was increased to 3.7 kW/m^2.

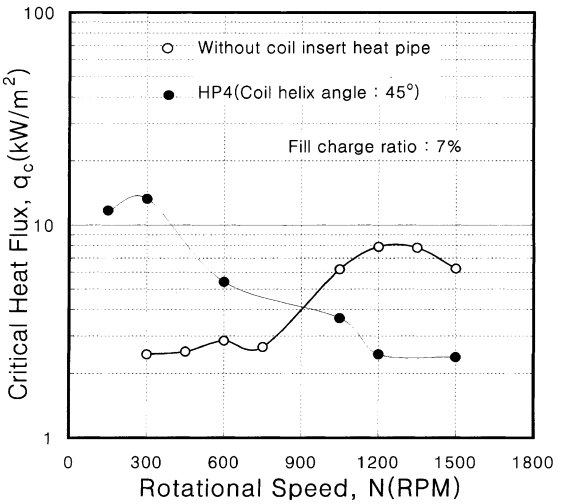

Fig. 12. Critical heat flux along with rotational speed for two types of heat pipes, without coil insert heat pipe [14] and with a coil insert HP4 having the same quantity of fill charge ratio.

design the present RHP. Fig. 12 shows the critical heat flux corresponding to 7% charge ratio as a function of rotational speed, for the two different conditions, i.e., without a coil and with a coil ($\alpha = 45°$). Overall trend indicates that the critical heat flux with a spiral coil is 300% larger than that of no coil in the pool flow. This may have resulted from the enhancement of the liquid flow rate, as observed in the flow visualization experiments. However, in the annular flow, the trend is reversed and the critical heat flux without a spiral coil is two times larger than that with a coil. Degradation of the critical heat flux in the case of using a coil can be explained by the fact that the spiral coil increases the flow resistance significantly since the film thickness is smaller than the coil diameter.

4. Conclusions

1. A spiral coil-inserted inside a rotating tube showed a pumping effect of the liquid film in the axial direction. Thus, the liquid is accumulated at the bottom of the right-hand side in the pool flow. However, in the annular flow, the pumping effect was diminished and a uniform liquid film was developed on the inner wall. As the charge ratio decreases, this trend seems to be more dominant. Also, a larger helix angle caused more enhanced pumping effect as well as earlier transition to the annular flow.
2. The condensing heat transfer coefficient was significantly enhanced in the pool flow due to the pumping effect of the coil. This might be caused by the reduction of the film thickness in the condenser. However, the enhancement of heat transfer coefficient was not observed any more once the liquid flow was subjected to the annular flow.
3. Decrease of the charge ratio resulted in the reduction of the film thickness in the condenser. Improvement of the condensing heat transfer coefficient with 15% charge ratio was 60–100% in the pool flow and 100% in the annular flow, when compared with that of 30 % charge. However, it is required to fill heat pipes with surplus working fluid since the decrease of the charge ratio causes degradation of the heat transport limitation.
4. The liquid flow in the condenser tends to be retarded if the film thickness is smaller than the coil diameter. Especially, degradation of the critical heat flux was observed to be significant for the spiral coil in annular flow regime, when compared with that for the case of no coil.

References

[1] V. Gray, The rotating heat pipe-a wickless hollow shaft for transferring high heat fluxes, ASME, 1969 Paper No. 69-HT-19.
[2] P.D. Dunn, D.A. Reay, in: Heat Pipes, fourth ed., Pergamon Press, Oxford, 1994.
[3] O. Brost, J. Unk, W.R. Canders, Heat pipes for electric motors, in: Proceedings of the Fifth International Heat Pipe Conference, 1984, pp. 359–364.
[4] F. Thoren, Heat pipe cooled induction motors, in: Proceedings of the Fifth International Heat Pipe Conference, 1984, pp. 365–371.
[5] B. Pokorny, F. Polasec, J. Schneller, Heat transfer in coaxial and parallel rotating heat pipes, in: Proceedings of the Fifth International Heat Pipe Conference, 1984, pp. 259–267.
[6] M.G. Semena, Yu.A. Khmelev, Hydrodynamic regimes of a liquid in a smooth-walled rotating heat pipe 1, Inzhenerno-Fizicheskii Zhurnal 43 (1982) 766–774.
[7] M. Katsuta, H. Kigami, K. Nagata, J. Sotani, T. Koizumi, Performance and characteristics of a rotating heat pipe, in: Proceedings of the Fifth International Heat Pipe Conference, 1984, pp. 126–132.
[8] J.S. Lee, C.J. Kim, E.T. Park, Y.K. Hwang, A fundamental study of operating characteristic for a rotating heat pipe, in: Proceedings of the Korean Society of Mechanical Engineers, 1995, pp. 610–615 (in Korean).
[9] W. Nakayama, Y. Ohtsuka, H. Itoh, T. Yoshikawa, Optimum charge of working fluid in horizontal rotating heat pipes, Heat Mass Transfer Rotating Machinery (1984) 633–644.
[10] R. Marto, M. Weigel, The Development of economical rotating heat pipes, in: Proceedings of the Fourth International Heat Pipe Conference, 1981, pp. 709–724.
[11] W. Nakayama, Y. Ohtsuka, T. Yoshikawa, The effect of fine surface structure on the performance of horizontal rotating heat pipes, in: Proceedings of the Fifth International Heat Pipe Conference, 1984, pp. 121–125.

[12] P.J. Marto, An analytical and experimental investigation of rotating heat pipes, NASA CR 130373, 1973.
[13] L. Lin, Cellular flow in a rotating heat pipe with stepped wall, Heat Recovery Syst. & CHP 11 (1) (1991) 63–68.
[14] A. Shimizu, S. Yamazaki, Helical guide-type rotating heat pipes, in: International Heat Pipe Conference, 1987, pp. 545–550.
[15] J.S. Lee, A study on the enhancement of condensate flow and the improvement heat transfer performance for a rotating heat pipe, Ph.D. dissertation, Sungkyunkwan University (in Korean), 1997.
[16] L.L. Vasiliev, V.V. Khrolenok, Heat transfer enhancement with condensation by surface rotation, Heat Recovery Syst. & CHP 13 (6) (1993) 547–563.